Identification of Damage Types in Carbon Fiber Reinforced Plastic Laminates by a Novel Optical Fiber Acoustic Emission Sensor

Fengming Yu, Qi Wu, Yoji Okabe, Satoshi Kobayashi, Kazuya Saito

IDENTIFICATION OF DAMAGE TYPES IN CARBON FIBER REINFORCED PLASTIC LAMINATES BY A NOVEL OPTICAL FIBER ACOUSTIC EMISSION SENSOR

Fengming Yu[1], Qi Wu[1], Yoji Okabe[1], Satoshi Kobayashi[2], and Kazuya Saito[1]

[1]*Institute of Industrial Science, the University of Tokyo, 4-6-1 Komaba, Meguro-ku, Tokyo 153-8505, Japan*

[2]*Graduate School of Engineering, Tokyo Metropolitan University, 1-1 Minami-Osawa, Hachioji, Tokyo 192-0397, Japan*

houmei@iis.u-tokyo.ac.jp

ABSTRACT

In this research, phase-shifted FBG (PS-FBG) sensor was employed to practical AE detection for carbon fiber reinforced plastic (CFRP) composite laminate. Firstly, we evaluated the characteristics of AE signals detected by this kind of sensor. Secondly, through the experiment and simulation concerning AE source orientation, quantitative information about the standard for discriminating the AE signals due to transverse cracks and delaminations was obtained. Finally, according to the standard, we identified the occurrence of those two damage types successfully in the actual AE detection under three point bending and tensile test.

KEYWORDS : *Optical fiber sensors, Acoustic emission, Composite laminate, Modal analysis.*

1 INTRODUCTION

Acoustic emission (AE) monitoring is considered as a kind of SHM methods for carbon fiber reinforced plastic (CFRP) composite laminates. In this material, AEs generated by crack occurrence have low energy and a broad frequency range. Hence, sensor with high sensitivities and broad bandwidth is one of key points for the practical application of the AE technology. PZT sensors have been being used as AE sensors. However, because this kind of sensor has bulk size and is easily broken by large displacement, it is difficult to be embedded in the CFRP composite laminates.

One kind of optical fiber sensors, FBG sensor, with flexibilities and small size, is possible alternative AE sensor [1]. However, the trade-off between high sensitivities and broad bandwidth limits the application of the sensor.

In order to solve these problems, Wu and Okabe [2, 3] tried to apply one special kind of FBG sensor, called phase-shifted FBG (PS-FBG), to AE detection.

1.1 PS-FBG & Balanced PS-FBG sensing system

At the centre of refractivity of PS-FBG, a narrow peak with sharp slope (Figure 1(b)) was generated due to a π phase shift which was inserted into the core of periodic grating area (Figure 1(a)). This narrow peak makes PS-FBG sensor possess both high sensitivity and broad bandwidth [4]. And the usefulness of the sensor for detecting ultrasonic wave in the CFRP laminates was verified [2].

Moreover, with taking advantages of PS-FBG sensor, Wu and Okabe developed a novel high sensitive sensing system, called balanced PS-FBG sensing system [3]. The configuration of this system is shown at Figure 1(c). In this system, based on edge filtering demodulation method, external cavity tunable laser (TLS) (Agilent, 81682A) was used as light source. Then, PS-FBG was connected with TLS through a circulator. The Reflected and transmitted light powers from PS-FBG propagate to port 1 and port 2 of a balanced photo detector (BPD) (New Focus, 2117) respectively. At the BPD, the light power will be transformed into electrical power. At the BPD, only AC electrical component caused by change of axial strains with the propagation of AE wave is passed

and DC component disappears. Additionally, due to the structure of BPD, the intensity noises produced by the laser are decreased. As a result, this novel system has very high sensitivities.

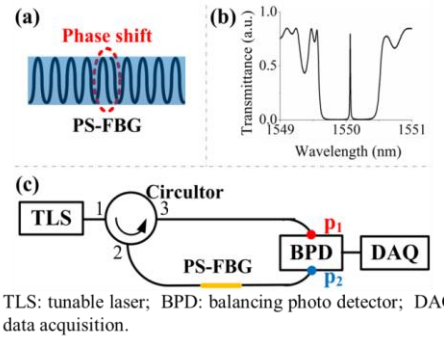

Figure 1: (a) the structure of PS-FBG, (b) the transmittance spectrum of PS-FBG, and (c) balanced PS-FBG sensing system.

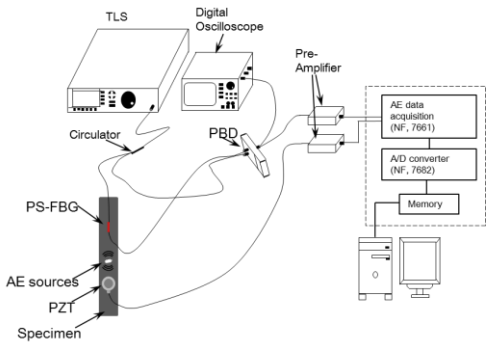

Figure 2: Sketch of acoustic emission experimental set-up.

The purpose of this paper is to verify that this balanced PS-FBG sensing system has the potential of SHM sensing system for practical AE detection in the CFRP laminate. To achieve this purpose, we have to evaluate the performance of PS-FBG sensor in identifying damage types [5].

In order to provide a better quantitative analysis of AE testing in which PS-FBG sensor was used, we adopted modal acoustic emission (MAE) technique in this research.

1.2 Modal acoustic emission method

MAE technique was established on the general theory of elastic waves in solids. Especially through the plate-like structure such as laminates, the AE wave shows characteristics of Lamb wave. According to the Lamb wave modes, particularly S_0 mode and A_0 mode, extracted from the AE signals, information of the AE source event can be extracted.

Based on the effects of AE source orientation on the AE modes, the standard of MAE method to identify damage types, such as transverse crack and delamination were built by using PZT sensors [6, 7, 8].

On the other hand, if PS-FBG sensor responses to the AE source orientations just like PZT sensor does, the standard for identifying damage types in the CFRP laminates should also be suitable in this research. However, on account of different sensing principles between PS-FBG sensors and PZT sensors, we have to conduct experiments to evaluate.

Hence, this paper is composed of three parts. Firstly, characteristics of AE signal detected by PS-FBG sensor was evaluated by comparison with the signal from PZT sensor. And then, experiment and FEM simulation concerning AE source orientation were conducted to obtain the quantitative information useful for identification of the damage types. Finally, based on the previous results, we tried to discriminate AE signals generated by transvers cracks and those by delaminations under the three points bending test and tensile test.

2 EXPERIMENTAL SETUP

2.1 Specimen preparation

All CFRP laminates specimens are manufactured from T700S/2500 (TORAY Inc.) carbon/epoxy prepreg system, and three different laminate configurations were used in this research. (1) In order to obtain the AE signals similar to results detected on the isotropic metal materials, CFRP quasi-isotropic laminate specimen $[45/0/-45/90]_{3S}$ ($200\times200\times3.5$ mm^3) was used in the experiment concerning about clarification of the features in AE signals detected by PS-FBG sensor. (2) Cross-

ply laminate $[0_2/90_2]_S$ (200×200×1.16 mm^3) was used in the AE source orientation experiment. The same laminate configuration with dimensions of 170×17×1.6 mm^3 was also used in the tensile test. The mechanical properties about this type of laminate were shown in Table 1. The reasons about the employment of this laminate configuration are as follows, firstly, it had been confirmed by preliminary tensile test that transverse cracks and delaminations can be generated in this laminate. Secondly, it is easy to relate actual AE signals to quantitative information for discriminating AE signals corresponding to the two fracture modes in AE source orientation experiment. (3) $[90/0]_S$ (176×19×0.6 mm^3) was used in three point bending test. This is because transverse cracks are easily generated at the surface of this specimen even under small loading.

Table 1: Mechanical properties of $[0_2/90_2]_S$ laminates

E_{11} (GPa)	E_{22} (GPa)	E_{33} (GPa)	G_{12} (GPa)	G_{23} (GPa)	G_{31} (GPa)	ρ (kg/m^3)
69.3	10	69.3	3.4	3.4	4.8	1530
ν_{21}	ν_{31}	ν_{32}				
0.067	0.036	0.4643				

2.2 AE data acquisition equipment

The output of the PS-FBG balanced sensing system and PZT sensors (Fuji Ceramics, 1045s) were ampified by pre-amplifier (NF corporation, 9917) and then recorded by an AE data acquisition unit (NF corporation, 7661). The PZT sensor is broad-band type with the frequency range from 0.2 MHz to 1.3 MHz. The gain of pre-amplifiers can be set from 10 dB to 40dB in the steps of 10 dB. The analogue AE signals were digitized through A/D convertors (NF corporation, 7682) with 12 bit resolution and maximum sampling rate of 10 MHz. All the waves in all channels of the AE system will be recorded by a trigger signal which one of all the AE signals crosses a pre-set threshold level. A schematic of the AE system is shown in Figure 2.

3 EXPERIMENTAL PROCEDURE AND RESULTS

3.1 Characteristics of AE signals detected by PS-FBG sensors

In order to evaluate the characteristics of AE signals detected by PS-FBG sensor, AE signals were generated by pencil lead break (PLB) on the laminate plate with the configuration of $[45/0/-45/90]_{3S}$. We also refer to results obtained by PZT sensor.

PZT sensor and PS-FBG sensor were mounted at the center point of plates and 100 mm away from the AE sources simulated by PLB on the surface of plate.

Figure 3 (a) and (b) show the temporal AE signals detected by PS-FBG sensor and PZT sensor respectively. The Fourier transform results corresponding to (a) and (b) were shown at Figure 3 (c) and (d) respectively.

Firstly, we investigated two AE signals shown in the figure 3 (a) and (b) in detail. Both temporal waveforms include S_0 mode and A_0 mode. The leading edges of the two basic lamb wave modes are indicated by the arrows on two results. The result shows that, as to the detection of S_0 mode component, PS-FBG has a much stronger responses than PZT sensor. On the other hand, PZT sensor has a much stronger response for A_0 mode than PS-FBG sensor.

This difference in waveforms may be caused by the difference in the sensing principles between two sensors. PS-FBG mainly detected the longitudinal strains caused by ultrasonic waves. Hence this kind of sensor is sensitive to the in-plane strain component which dominates in the S_0 mode. On the contrary, PZT sensor is sensitive to out-of-plate component, so that it has a much stronger responses to A_0 mode. Additionally, unlike PS-FBG, depending on frequency, PZT sensors not only detect strain, but also detect displacements, acceleration and so on.

Secondly, we investigated the signals on the frequency domain. Figure 3 (d), the result of PZT sensor, shows that a peak occurred around the 0.2 MHz in the spectral response. By contrast, Figure

3 (c) indicates that PS-FBG has a broad bandwidth response even in the frequency field below 0.2 MHz. It means that PS-FBG has much more broad bandwidth than PZT sensor, which is possible to be used for frequency analysis with much more reliability.

This experiment indicates that, because of the high sensitivities, PS-FBG sensor is eligible for providing quantitative analysis to AE testing as well as PZT sensors. However, AE signals detected by two sensors respectively are very different due to the different sensing principles. It means that the standard built under employment of PZT sensors cannot be directly applied. Therefore, in this research, before conducting the practical AE detections, we should discuss the standard for identifying the damage types that is suitable for PS-FBG sensors. Hence, we conducted the next experiment about AE source orientation.

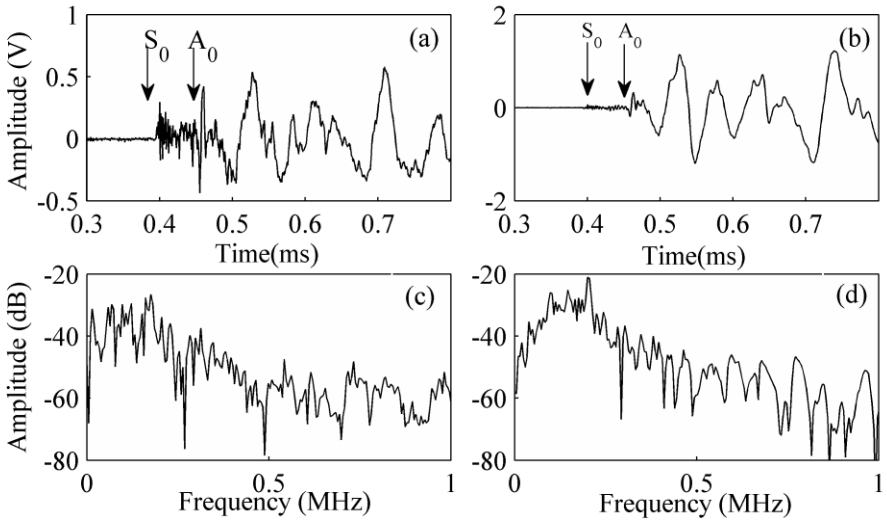

Figure 3: Response to PLB with 45 degree on the CFRP $[45/0/-45/90]_{3s}$ laminates: (a) Received wave by the PS-FBG. (b) Received wave by the PZT. (c) Fourier spectrum of (a). (d) Fourier spectrum of (b).

3.2 Effects of AE source orientation

From the view of MAE method, the standard for discriminating the AE signals generated by transverse crack or delamination involves the difference in effects of AE source orientations [8]. The relationship between damage types and source orientation is illustrated as Figure 4 in a side view of a cross-ply specimen. In the Figure 4 (a) and (b) are schematic of transverse cracking. Particularly, in the (a), the motion of the transverse crack surfaces is parallel to the plane of the specimen and, here, we put this kind of damage type has the source orientation with 0 degree. It can be expected that matrix crack will generate AE waves which an in-plane mode, S_0 mode dominates. By contrast, Figure 4 (c) shows that the delamination has a source orientation with 90 degree, so that it is supposed that this damage type generates the AE with dominant A_0 mode.

In order to verify the above assumption and responses of PS-FBG sensor to AE source orientation, we used PLB at 15, 30, 60, 90 degrees with respect to the neutral surface of the $[0_2/90_2]_S$ laminate to simulate the AE sources with different orientations. Here, for the case of 15, 30 and 60 degree lead breaks, slots were machined at the edge of plate. PLB at the 90 degree was conducted on the surface of the plate directly. At each angle, the break was repeated 22 times to ensure the experimental reproducibility. PS-FBG sensor and PZT sensor were place 90 mm away from the AE source, and the orientation of PS-FBG is parallel to fibers in the surface of laminate.

To obtain quantitative results, E/F ratio [8] was introduced to evaluate the effects of different angles. E/F ratio is the ratio of the peak amplitude of A_0 mode to that of S_0 mode. Additionally, mode separation was conducted according to the analytical result regarding to arrival times of S_0 mode and A_0 mode based on the group velocities of two modes calculated by a commercial software DIPERS.

3.2.1 Experimental results

As an experimental result, the E/F ratio map was shown in Figure 5. Firstly, according to the result, it was found that, following with the increasing degrees, both PZT sensor and PS-FBG sensor have a similarly monotonous decreasing E/F ratio. Hence, we have to say that PS-FBG sensor has the same performance for the effects of AE source orientation just like PZT sensor. Based on the relationship between fracture modes and source orientations, the E/F ratio indicates that in the laminate plate, S_0 mode dominates in the AE generated by transverse crack, on the contrary, A_0 mode dominates in the AE generated by delamination.

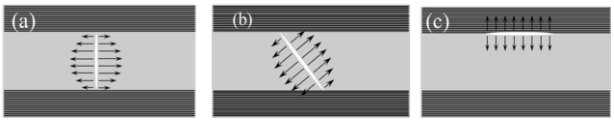

Figure 4: Schematic illustration of AE source orientation caused by (a) transverse cracking (0 degree), (b) transverse cracking (30 degree), (c) delamination (90 degree).

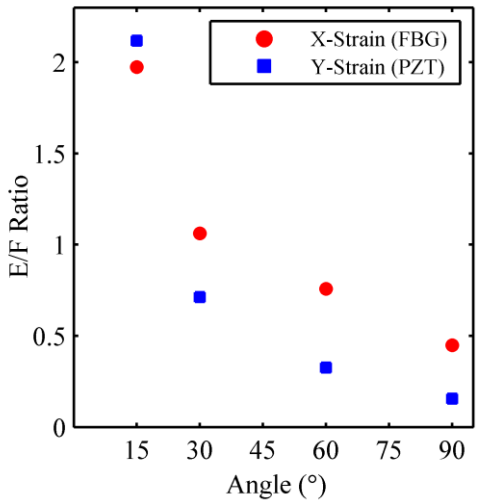

Figure 5: E/F ratio measured by PS-FBG and PZT sensor at each angle of PLB.

3.2.2 Validation with FEA

At the experiment, some factors such as the thickness of the laminate plate, and the reflection wave may bring about errors in the E/F ratio. Hence, it is necessary to validate the experimental results under Numerical simulations

Numerical simulations were conducted with 2D FEA using LS-DYNA software. The CFRP laminate (longitudinal length: 500 mm, thickness: 1.2 mm) were modeled with shell elements for 2D plane strain. The element dimensions in the CFRP laminate were 0.1 mm×0.1 mm. In order to prevent the reflection of AE, the length of the laminate was set much longer than the actual specimen. The schematic of the model is shown in Figure 6 (a). The mechanical properties of the CFRP are listed in table 1.

We used monopole source to simulate the released original signals from PLB. The time behaviour of the source obeys the cosine bell with a rise-time of 0.8 μs, and transient time of 1.3 μs. The temporal curve was shown in Figure 6 (b).

The input point is set at combination of neutral axis and edge side as shown in Figure 6(a). We used different angles of input resource to simulate the different degrees between PLB and the surface of the laminate plate.

The temporal strain wave in the longitudinal direction (X-axis) was obtained as received wave in PS-FBG at the receiving point on the surface of the laminates. Results of PZT sensor refer to the strains along the Y-axis. E/F ratio was also used to evaluate the effects of AE source orientation. Then, arrival times of two modes, A_0 mode and S_0 mode, were set at the same as the experiment. The analytical result shown in the Figure 7 indicates that E/F ratio decreases with increasing angles. It coincides with the experimental result. Hence, we validated the effectiveness of results obtained in the experiment.

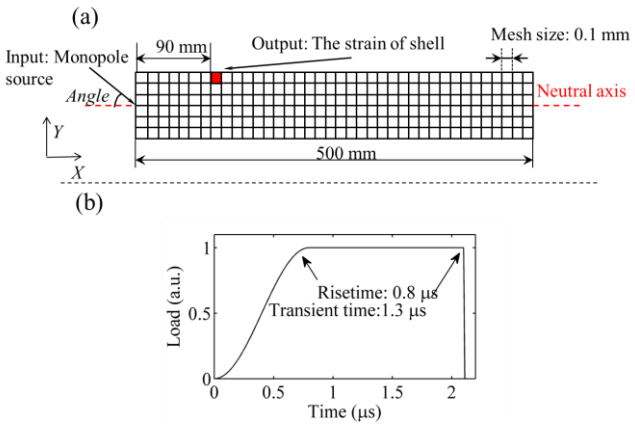

Figure 6: (a) Dimensions and configuration of FEM model for numerical investigation of influence on AE mode due to source orientation. (b) Monopole source.

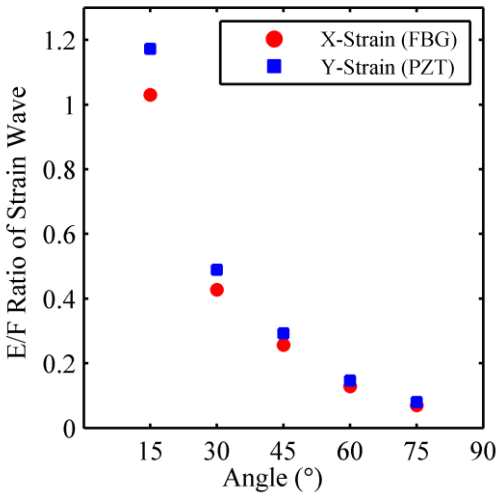

Figure 7: E/F ratio of simulated strain waveforms in the X-axis (PS-FBG) and Y-axis (PZT).

3.3 Practical AE detection

Based on the results obtained in the previous chapter, we tried to discriminate the AE signals generated by transverse cracks and delaminations at the actual AE detection under the three point bending test and tensile test.

3.3.1 Three point bending test

Firstly, the three point bending test was implemented using a three point bending test jig and small material testing machine. The $[90/0]_S$ specimen was used in this test. The position of loading pin and supporting pins were shown in Figure 8(a). The stroke of loading pin was provided by a small size experimental machine, and the cross head speed was set to 2 mm/min.

PS-FBG sensor and three PZT sensors were placed on the specimen in the arrangement shown schematically in Figure 8(a). Sensors was mounted by couplant and tape. PS-FBG sensor was located at the position that was far away 60 mm from the loading pin. At the same position on opposite sides of the specimen, a PZT sensor was mounted as reference sensor, we called this sensor as PZT1. The other sensor pair including PZT2 and PZT3 was symmetrically mounted about the loading pins. This PZT sensor pair was used to identify S_0 mode components and A_0 mode components included in the AE wave. According to the symmetric (S mode) and asymmetric (A mode) features, S_0 mode components detected by the sensor pair will appear the same phase, on the contrary, A_0 mode will appear with the opposite phase.

21 AE hits were generated during the experiment, and we found the characteristics of AE signals were similar. Hence, we only showed one representation signal in the Figure 9.

From Figure 9(a), we confirmed that PS-FBG sensor can detect the practical AE signals. Then, we found that S_0 mode dominated in this AE wave according to (c). After testing, we confirmed under the microscope that only transverse crack happened. Hence, we have to say that, this signal was generated by transverse crack. This result also coincides with that of the transverse crack obtained at the AE source orientation experiment.

However, because of the small power of the testing machine, we cannot produce the delamination at the three point bending test. Hence, we carried out the tensile test.

3.3.2 Tensile test

Tensile test was conducted using a tensile test machine (AG-50kNG, Shimadzu Inc.). The $[0_2/90_2]_S$ specimen with aluminum tabs was clamped between wedge grips and, the cross-head speed was set to 1 mm/min. Strain gage were used to record the strain during testing.

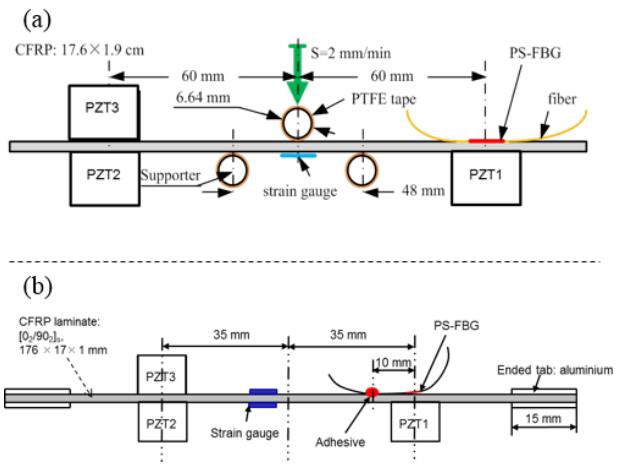

Figure 8: Schematic illustration of (a) three point bending test and (b) tensile test.

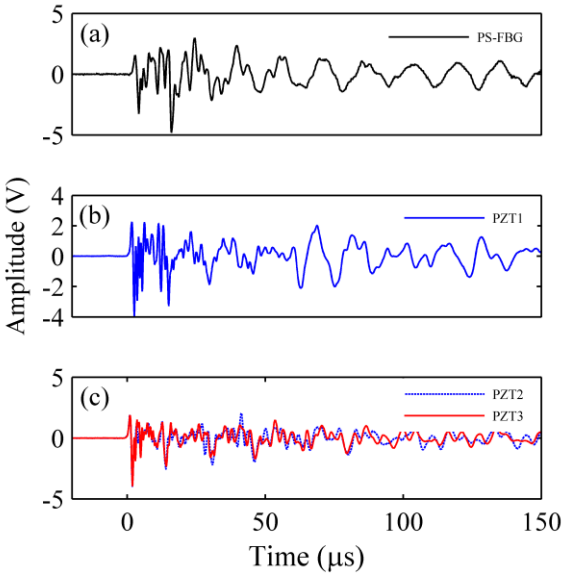

Figure 9: AE temporal waveforms detected under three point bending test by (a) PS-FBG, (b) PZT1 and (c) PZT2 & PZT3.

The distribution of sensors was similar with three point bending test, except for the gluing method of PS-FBG sensor. It was shown schematically in Figure 8(b). Different from the three point bending test, in order to avoid the quasi-static strain which have effects on the AE detection of PS-FBG sensor, we used adhesive to glue the part of fiber at the external point next to the PS-FBG sensor rather than the part of sensor. The distance from the adhesive point to the PS-FBG sensor was set to 10 mm which was a reasonable distance verified by the experiment.

At this experiment, a reasonable threshold and gain of preamplifier was set determined for the preliminary test. The specimen was tensile loaded until to 1.3% of strain, and about 150 AE hits were generated during this process. Observation under the microscope verified that transverse crack and delaminations occurred during the experiments.

Figure 10 and Figure 11 showed two typical AE signals generated by transverse crack and delamination respectively.

Figure 10 (c) showed that S_0 mode dominated in the AE signals, which was the same with results obtained in three point bending test. Hence we identified this result was generated by transverse cracks. Figure 10 (a) and (b) also indicated AE signals detected by PS-FBG sensor and PZT1 had the similar characteristics that S_0 mode dominates.

On the contrary, Figure 11 (c) shows that A_0 mode dominates in the AE signals. According to the results obtained at the experiment about the AE source orientation, this AE wave with A_0 mode was generated by the delamination. At the beginning of time range from 0 μs to 50 μs, the overlap part of two AE signals can show the existence of S_0 mode, then, A_0 mode arrived with a large power which resulted in over the available measurement electrical range of AE acquisition system. From the results shown in the Figure 11 (c), S_0 mode had a high frequency compared with A_0 mode, which coincide with other researches [5, 8]. Then, we paid attention to the AE signals detected by PS-FBG sensor shown in the Figure 11 (a).We found that high frequency components also appeared earlier than low frequency components, it means at beginning part of AE wave contain S_0 mode and A_0 mode arrived latter. Additionally, the peak amplitude of A_0 mode components is clearly larger than that of S_0 mode. In other words, the AE signal detected by PS-FBG sensor also shows the characteristics of AE generated by delamination.

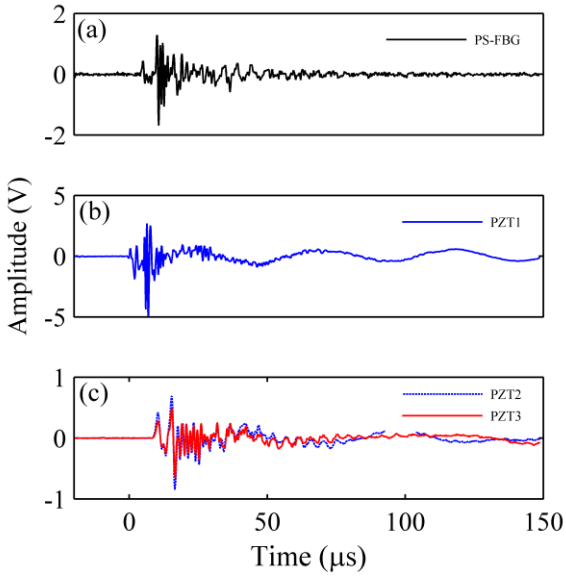

Figure 10: AE signals due to transverse cracks detected under tensile test by (a) PS-FBG, (b) PZT1, and (c) PZT2 & PZT3.

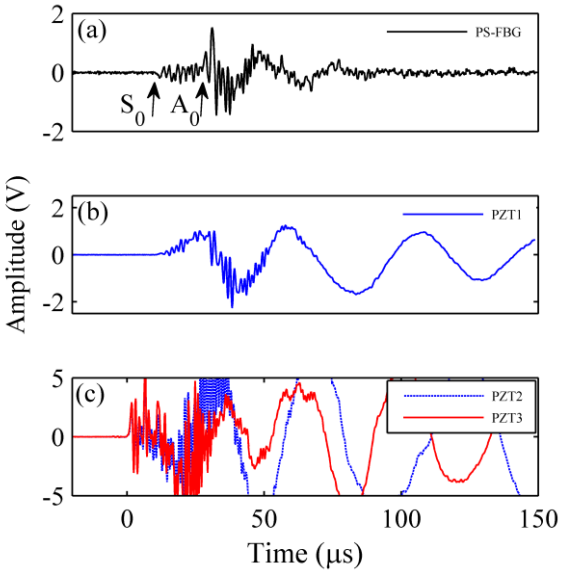

Figure 11: AE signals due to delamination detected under tensile test by (a) PS-FBG, (b) PZT1, and (c) PZT2 & PZT3.

4 CONCLUSIONS

This research indicates that PS-FBG sensor as AE sensor is eligible for providing quantitative investigation to the AE testing. Then, we evaluated quantitatively the responses of PS-FBG sensor to the AE source orientation with the same trend as the PZT sensor. At the same time, the standard for discriminating the AE signals generated by transverse crack and delamination was also verified. In the three point bending test, it was comfirmed that S_0 mode dominates in the AE signals due to transverse crack. On the other hand, in the tensile test, not only were AE signals with S_0 mode found, but also the AE signals dominated by A_0 mode appeared. In accordence with features of AE signals, we identified the occurrance of transverse crack and delamination.

Hence, through this research, we believe that PS-FBG sensor has the potential of being applied to pratical AE detection of CFRP composite laminate.

REFERENCES

[1] G. Wild. Acousto-Ultrasonic Optical Fiber Sensors: Overview and State-of-the-art. *IEEE Sensors Journal*, 8:1184–1193, July 2008.

[2] Q. Wu and Y. Okabe. Ultrasonic Sensor Employing Two Casecaded Phase-shifted Bragg Gratings suitable for multiplexing. *Optics letters*, 37:3336-3338, August 2012.

[3] Q. Wu, Y. Okabe. High-sensitivity Ultrasonic Phase-shifted Fiber Bragg Grating Balanced sensing system. *Optics express*, 20:28353-28362, December 2012.

[4] A. Rosenthal, D. Razansky, V. Ntziachristos. High-sensitivity Compact Ultrasonic Detector Based on A Pi-phase-shifted Fiber Bragg Grating. *Optics letters*, 36: 1833-1835, May 2011.

[5] J. J. Scholey, P. D. Wilcox, M. R. Wisnom, M. I. Friswell. Quantitative Experimental Measurements of Matrix cracking and delamination using acoustic emission. *Composites: Part A*, 41: 612-623, May 2010.

[6] M. R. Gorman, W. H. Prosser. AE Source Orientation by Plate Wave Analysis. *Journal of acoustic emission*, 9: 283-288, 1991.

[7] W.H. Prosser, K. E. Jackson, S. Kellas, B. T. Smith, J. Mckeon, A. Friedman. Advanced, Waveform Based Acoustic Emission Detection of Matrix Cracking in Composites. *Material evaluation*, 53: 1052-1058, September 1995.

[8] M. Surgeon, M. Wevers. Modal Analysis of Acoustic Emission Signals from CFRP laminates. *NDT&E International*, 32: 311-322, September 1999.